Stem Cell Reports, Volume *15*

Supplemental Information

Estrogen Receptor β Controls Muscle Growth and Regeneration in Young Female Mice

Daiki Seko, Ryo Fujita, Yuriko Kitajima, Kodai Nakamura, Yuuki Imai, and Yusuke Ono

Figure S1

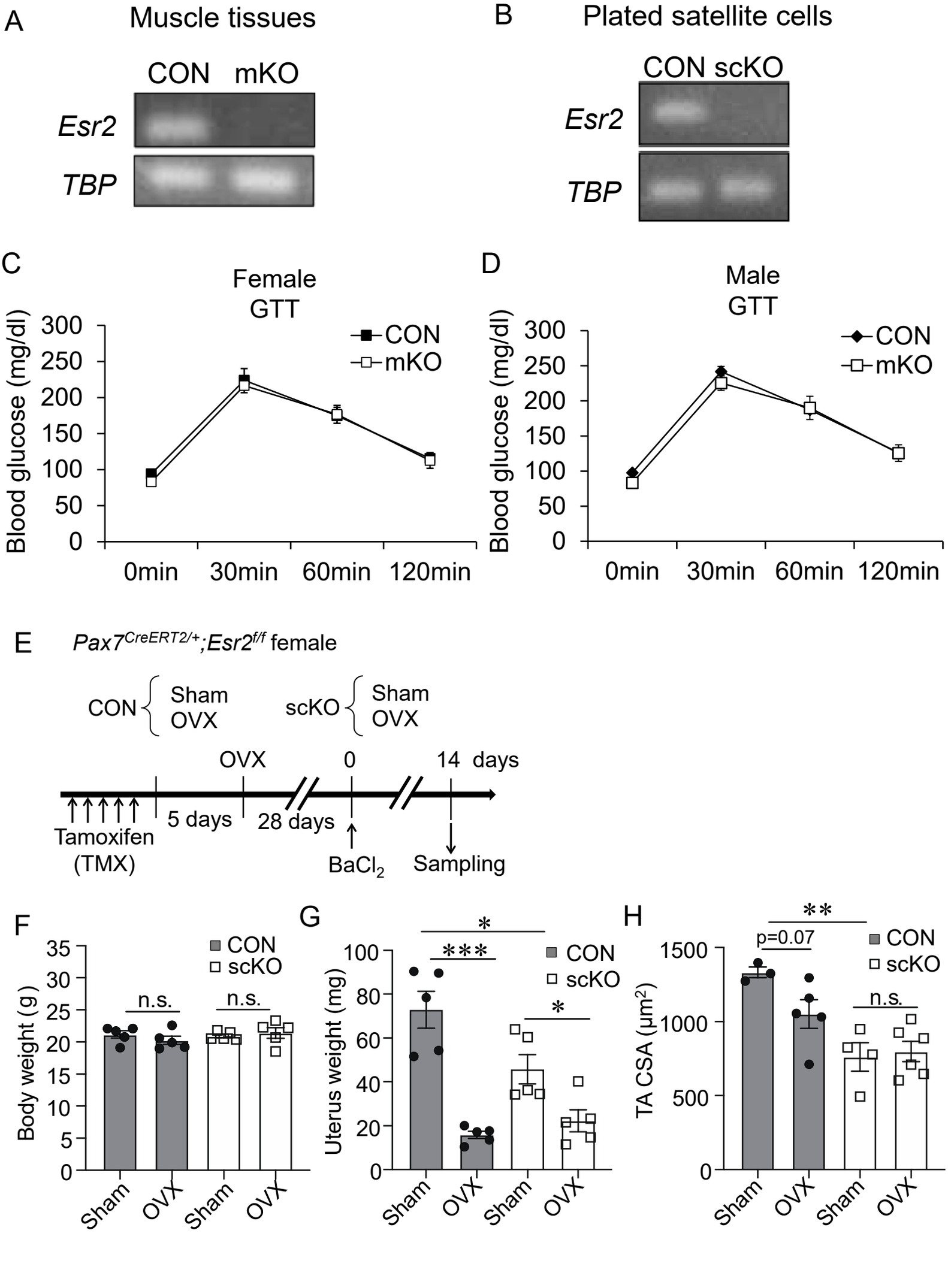
A
Muscle tissues
CON mKO
Esr2
TBP
B
Plated satellite cells
CON scKO
Esr2
TBP
C
Female GTT
Blood glucose (mg/dl)
CON
mKO
0min 30min 60min 120min
D
Male GTT
Blood glucose (mg/dl)
CON
mKO
0min 30min 60min 120min
E
Pax7CreERT2/+;Esr2f/f female
CON Sham OVX
scKO Sham OVX
OVX 0 14 days
5 days 28 days
Tamoxifen (TMX)
BaCl2
Sampling
F
Body weight (g)
CON scKO
n.s. n.s.
Sham OVX Sham OVX
G
Uterus weight (mg)
* *** *
CON scKO
Sham OVX Sham OVX
H
TA CSA (μm2)
** p=0.07 n.s.
CON scKO
Sham OVX Sham OVX

Figure S1. OVX does not further exacerbate the impaired muscle regeneration in ERβ scKO mice

(A-B) Representative images of RT-PCR products for *Esr2* in TA muscles (A) or satellite cells (B).

(C-D) Glucose metabolism is not altered in muscle-specific ERβ inactivated mice. (C) Glucose tolerance test was performed in female CON and mKO mice (CON, n=5 mice; mKO, n=5 mice). (D) Glucose tolerance test was performed in male CON and mKO mice (CON, n=3 mice; mKO, n=3 mice). Data represent means ± standard error of the mean. not significant. Student's t test.

(E-H) OVX-induced estrogen insufficiency does not further exacerbate the reduced myofiber sizes in ERβ scKO mice. (E) TMX was injected intraperitoneally into *Esr2*$^{f/f}$ (CON) mice and *Pax7*$^{CreERT2/+}$*;Esr2*$^{f/f}$ (scKO) mice. Mice were ovariectomized (OVX) for 28 days at day 5 following TMX injection and sacrificed at day 14 following $BaCl_2$ injection into TA muscle. (F) Body weight (Sham-CON, n=5 mice; OVX-CON, n=5 mice; Sham-CON, n=5 mice; OVX-scKO, n=6 mice). (G) Uterus weight (Sham-CON, n=5 mice; OVX-CON, n=5 mice; Sham-CON, n=5 mice; OVX-scKO, n=6 mice). (H) CSA of TA muscle (Sham-CON, n=3 mice; OVX-CON, n=5 mice; Sham-CON, n=4 mice; OVX-scKO, n=6 mice). Data represent means±standard error of the mean. *, p<.05; **, p<.01; ***, p<.001; n.s., not significant, one-way ANOVA followed by Bonferroni's multiple comparison tests.

Figure S2

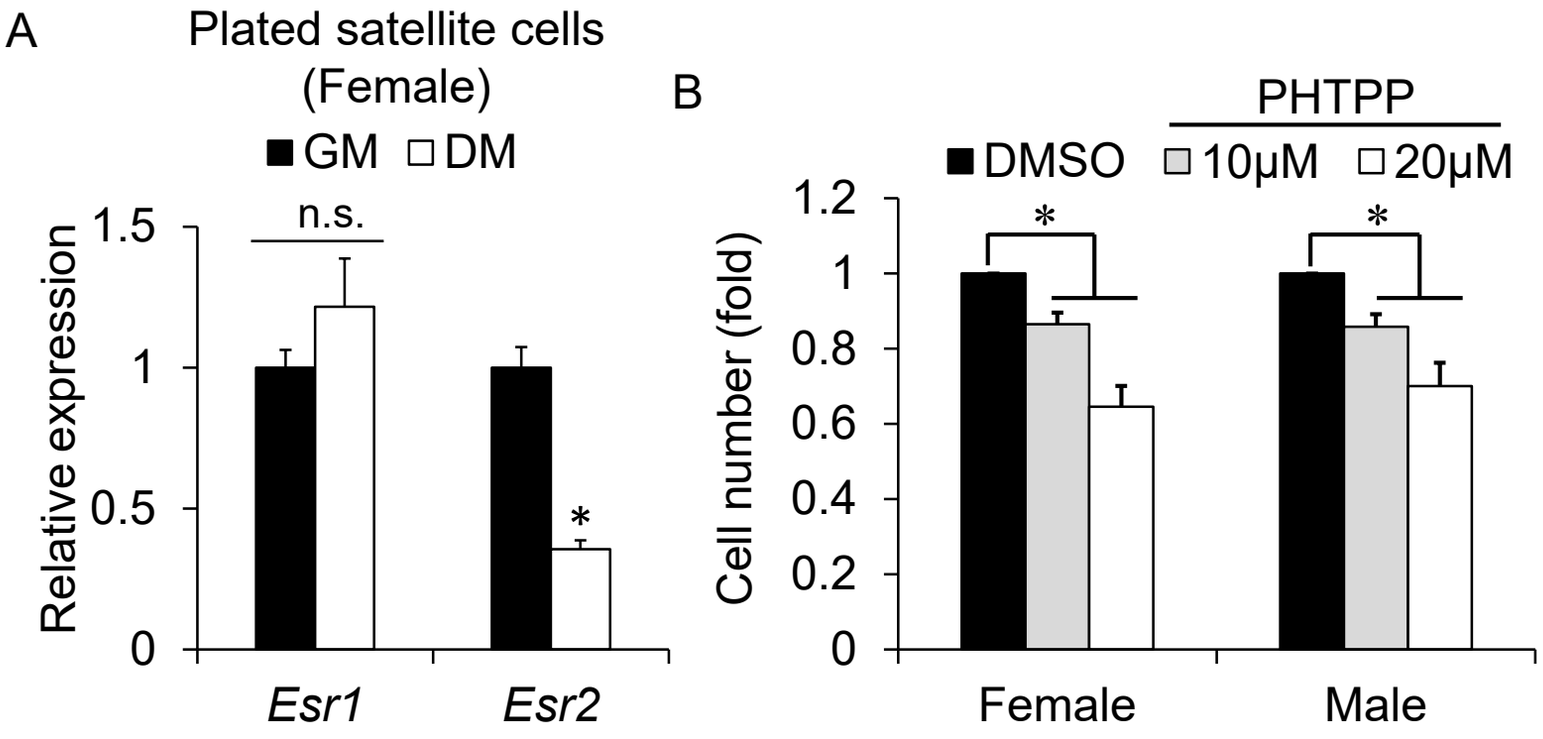

Figure S2. Satellite cell proliferation is attenuated by treatment with an ERβ selective antagonist

(A) Q-PCR analysis for the expression of *Esr2* and *Esr1* in primary satellite cells maintained in GM and DM culture conditions (n=3 mice, each group).

(B) The number of satellite cells treated with PHTTP, a selective antagonist of ERβ (n=3 mice, each group).

Data represent means ± standard error of the mean. *, p<.05; n.s., not significant. Student's t test.

Figure S3

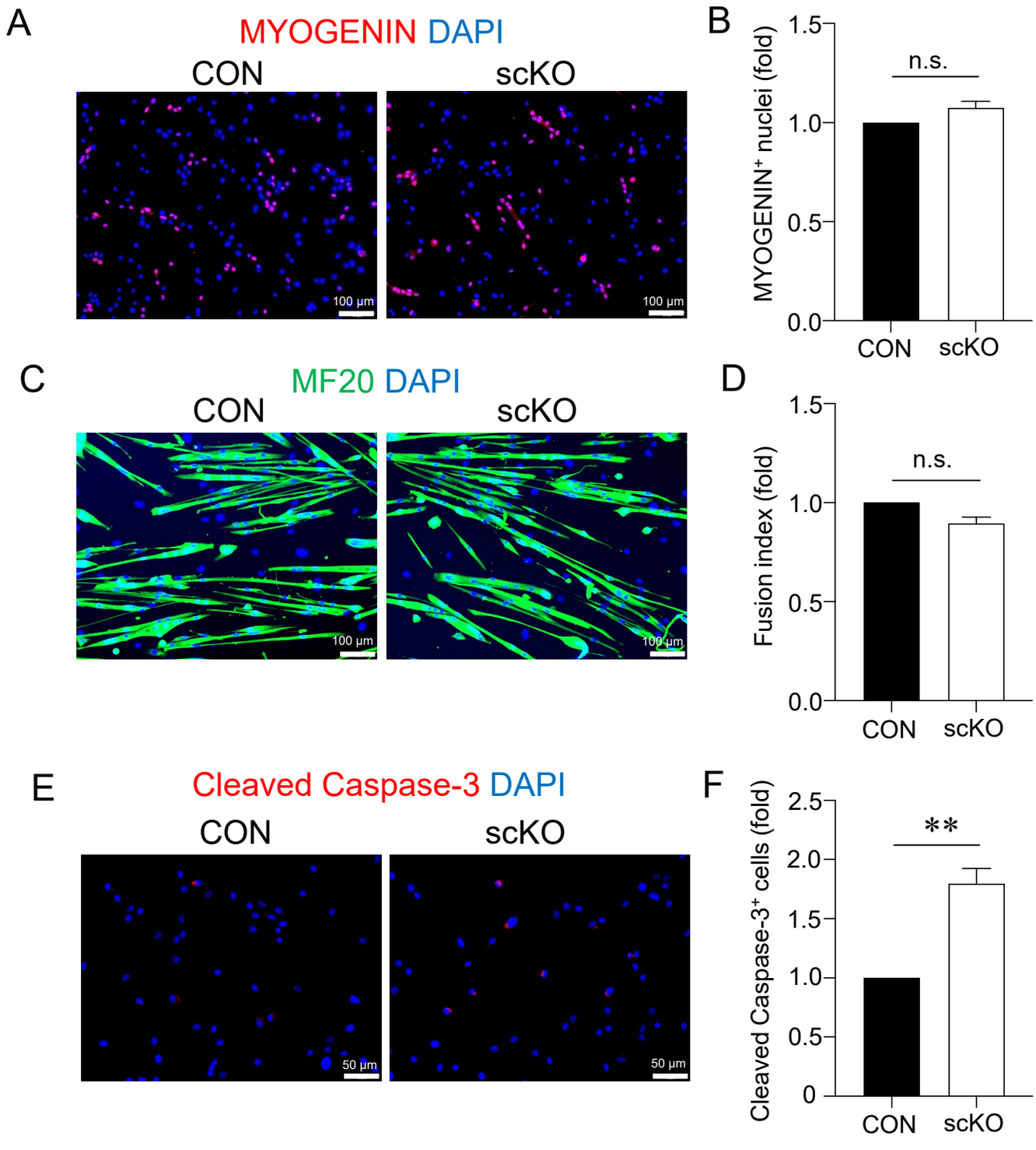

Figure S3. Effects of ERβ deletion on apoptosis and differentiation of satellite cells

(A-F) Satellite cells were isolated from *Pax7*$^{CreERT2/+}$*;Esr2*$^{f/f}$ mice and ERβ was inactivated by 4OH-TMX treatment as shown in Fig.4A.

(A-B) Immunofluorescence for MYOGENIN in ERβ-deleted satellite cells in GM. Representative images (A) and quantitative data for MYOGENIN$^+$ nuclei per DAPI$^+$ nuclei (B). n=3 mice, each group.

(C-D) Myogenic differentiation was induced in ERβ-deleted satellite cells in DM. (C) Representative images of immunofluorescence for MF20. (D) Myogenesis was evaluated by fusion index (the relative number of MF20$^+$ myotubes that contain more than 5 nuclei per MF20$^+$ nuclei). n=3 mice, each group.

(E-F) Immunofluorescence for cleaved Caspase-3 in ERβ-deleted satellite cells in GM. Representative images (E) and quantitative data for cleaved Caspase-3$^+$ nuclei per DAPI$^+$ nuclei (F). n=3 mice, each group.

Data represent means ± standard error of the mean. **, p<.01; n.s., not significant. Student's t test.

Figure S4

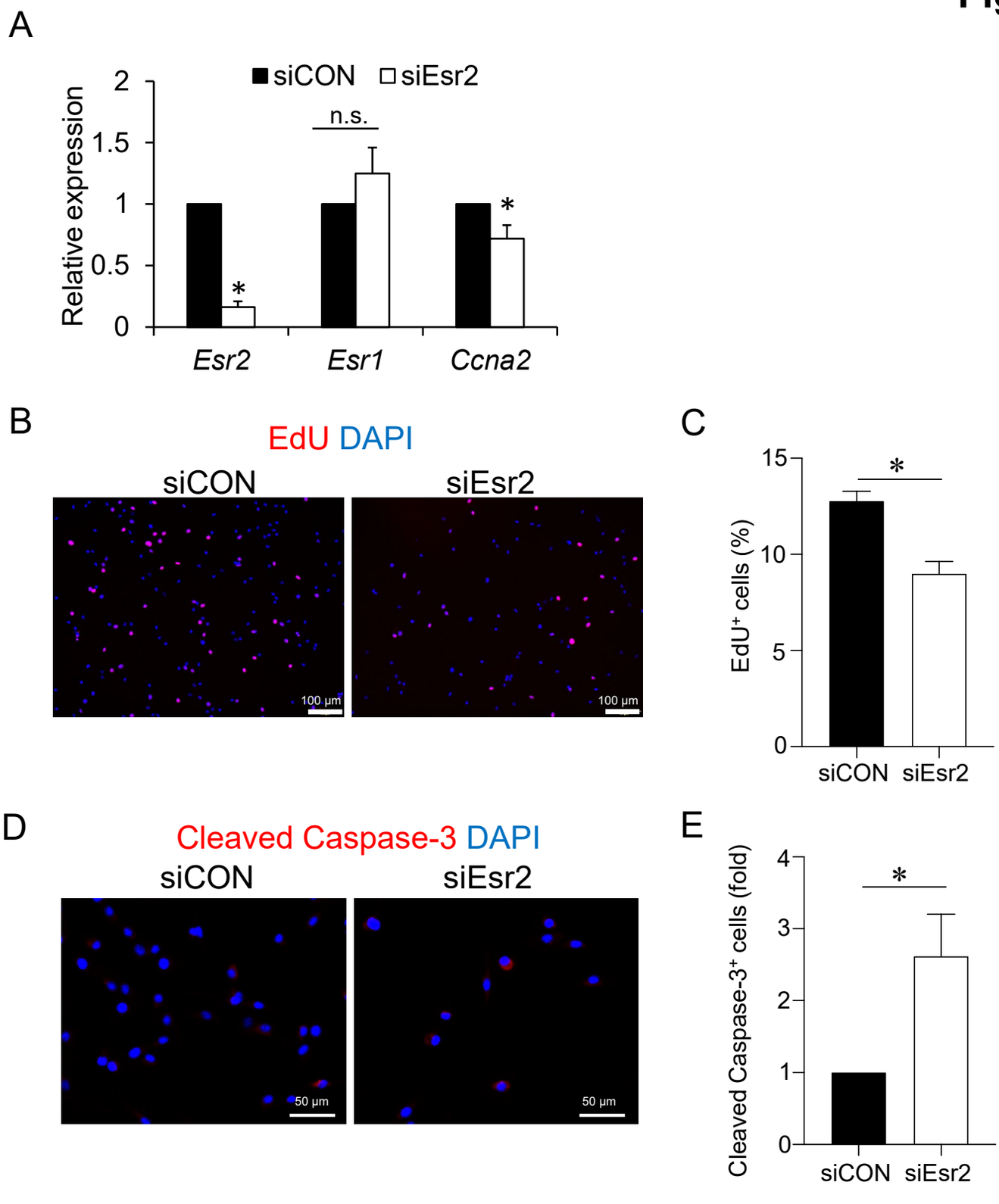

Figure S4. Knockdown of ERβ suppresses cell cycle entry and induces apoptosis in satellite cells

(A-E) Effects of siRNA-mediated knockdown of ERβ on satellite cells in culture.

(A) Q-PCR analysis for the expression of *Esr2*, *Esr1*, and *Ccna2* in siRNA-transfected satellite cells. n=3 mice, each group.

(B-C) EdU staining of satellite cells. Representative images (B) and quantitative data for EdU^+ nuclei per $DAPI^+$ nuclei (C). n=4 mice, each group.

(D-E) Immunofluorescence of cleaved $Caspase\text{-}3^+$ satellite cells. Representative images (D) and quantified data (E). n=3 mice, each group.

Data represent means ± standard error of the mean. *, $p<.05$; n.s., not significant. Student's t test.

Supplemental Experimental Procedures

Antibodies and reagents

Mouse anti-Type IIa myosin heavy chain (MyHC) (SC-71) and mouse anti-Type IIb MyHC (BF-F3) antibodies were obtained from Deutsche Sammlung von Mikroorganismen (Braunschweig, Germany). Mouse anti-myosin heavy chain (MF20) antibody was obtained from R&D Systems (Minneapolis, MN). Mouse anti-PAX7, mouse anti-MYOGENIN, and rabbit anti-MYOD antibodies were purchased from Santa Cruz Biotechnology (Santa Cruz, CA). Rat anti-laminin α2 antibody was obtained from Alexis (San Diego, CA, USA). Rabbit anti-M-Cadherin and rabbit anti-Cleaved Caspase-3 antibodies were purchased from Cell Signaling Technology (Beverly, MA). Goat anti-collagen Type I antibody was purchased from Southern Biotech (Birmingham, AL, USA). The mounting medium containing 4′,6-diamidino-2-phenylindole for nuclear staining and a Mouse On Mouse (M.O.M.) kit were purchased from Vector Laboratories (Burlingame, CA, USA). Tamoxifen (TMX) and 4-hydroxy TMX (4OH-TMX) were purchased from Sigma-Aldrich (St. Louis, MO, USA). A selective antagonist of ERβ, 4-(2-phenyl-5,7 bis(trifluoromethyl)-pyrazolo[1,5-a] pyrimidin-3-yl)-phenol

16 (PHTPP), was purchased from Sigma-Aldrich. The Click-iT ™ EdU Cell Proliferation Kit was
17 purchased from Thermo Fisher Scientific (Waltham, MA).
18
19 **Muscle functional tests i*n vivo***
20 Mice 10- to 13-weeks of age were subjected to a low-intensity, run-to-exhaustion protocol on
21 a motorized treadmill as previously described (Fujita et al., 2018). The mice were familiarized
22 with the treadmill (Muromachi Kikai, Tokyo, Japan) for 10 min at 10 m/min for 2 consecutive
23 days. The next day, each mouse were run at 10 m/min for 30 min, 11 m/min for 15 min, and
24 12 m/min for 15 min with a 15° incline. Finally, the speed was incrementally increased by 1
25 m/min every 10 min until the mouse exhibited exhaustion. The endpoint was achieved when
26 the mouse sat on the shock grid at the back of the treadmill for longer than 5 s.
27 Whole-limb grip strength was measured using a Grip Strength Meter for mice
28 (Columbus Instruments, Columbus, OH, USA) as previously described (Fujita et al., 2018).
29 Peak tension (in newtons) was recorded when the mouse released its grip. Two sets of 10
30 successive measurements were performed for each mouse and the mean maximum strength
31 in each set of experiments was used for data analysis.

Glucose tolerance test

A glucose tolerance test was performed by intraperitoneal glucose injection (1 g/kg body weight) after overnight food withdrawal (16 h). Blood-glucose concentrations were measured using an Accu-Chek meter (Roche, Basel, Switzerland) before (0 min) and 30, 60, and 120 min after glucose injection.

Myofiber and satellite cell isolation and culture

EDL muscles were isolated and digested with type I collagenase as previously described (Ono et al., 2015). Satellite cells were obtained from isolated myofibers and cultured in GM (Dulbecco's modified Eagle's medium (DMEM) supplemented with 30% fetal bovine serum, 1% chicken-embryo extract, 10 ng/mL basic fibroblast growth factor, and 1% penicillin-streptomycin) at 37°C in a 5% CO_2 atmosphere. Myogenic differentiation was induced in DM (DMEM supplemented with 5% horse serum and 1% penicillin-streptomycin) at 37°C in a 5% CO_2 atmosphere. For floating culture, isolated myofibers associated with satellite cells were

47 cultured in plating medium (PM; DMEM supplemented with 10% horse serum, 0.5% chick
48 embryo extract, and 1% penicillin-streptomycin) at 37°C in a 5% CO_2 atmosphere.
49
50 **Immunostaining**
51 Immunocytochemistry of satellite cells associated with myofibers was performed as
52 previously described (Ono et al., 2015). Samples were fixed with 4% paraformaldehyde,
53 blocked/permeabilized with phosphate-buffered saline containing 0.3% Triton X100 and 5%
54 goat or porcine serum for 20 min at room temperature, and incubated with primary antibodies
55 at 4°C overnight. TA muscle tissues were immediately frozen in 2-methylbutane cooled in
56 liquid nitrogen and stored at −80°C before being cryosectioned. Hematoxylin and eosin
57 (H&E) staining and Oil Red O staining were performed as previously described (Fujita et al.,
58 2018). Frozen cross-sections of TA muscle were fixed with 4% paraformaldehyde, blocked
59 with M.O.M., and incubated with primary antibodies at 4°C overnight. All immunostaining
60 samples were visualized using appropriate species-specific Alexa Fluor 488 and/or 568
61 fluorescence-conjugated secondary antibodies (Thermo Fisher Scientific, Waltham, MA).
62 Samples were viewed on an Olympus microscope IX83 (Olympus, Tokyo, Japan) or a

CellInsight CX5 (Thermo Fisher Scientific). Digital images were acquired and quantified with a DP80 camera using cellSens software (Olympus). Images were optimized globally and assembled into figures using Adobe Photoshop.

siRNA transfection

Transfection of siRNA was performed as previously described (Ono et al., 2011). Isolated satellite cells were seeded in six-well plates and transfected with siRNA at 30-40% confluence. MISSION siRNA (Sigma-Aldrich) were diluted in OptiMEM (Thermo Fisher Scientific) to 2-10 pmol per well and incubated with RNAiMAX (Thermo Fisher Scientific) diluted in OptiMEM according to the manufacturer's instructions. The following siRNA sequences were used: Esr2 siRNA (SASI_Mm01_00185612 (siRNA #1); SASI_Mm02_00317914 (siRNA #2). A control siRNA sequence selected by Sigma-Aldrich was used.

Q-PCR

Total RNA was extracted from cultured satellite cells or muscle tissues using an RNAeasy Kit (Qiagen, Hilden, Germany) or an ISOGEN II (Nippon Gene, Tokyo, Japan), respectively.

cDNA was prepared with a ReverTra Ace kit with genomic DNA remover (Toyobo, Tokyo, Japan). Q-PCR was performed using a THUNDERBIRD SYBR qPCR mix and CFX96 Touch real-time PCR detection system (Bio Rad, Tokyo, Japan). Primer sequences were as follows: TATA box binding protein (TBP) as a normalizer (F 5'-CAGATGTGCGTCAGGCGTTC-3' and R 5'-TAGTGATGCTGGGCACTGCG-3'); *Esr1* (F 5'- TTATGGGGTCTGGTCCTGCG -3' and R 5'-TCCGTATGCCGCCTTTCATCA -3'); *Esr2* (F 5'- GCCAACCTCCTGATGCTTCT-3' and R 5'- TCGTACACCGGGACCACAT-3'); *Ccna2* (F 5'- CCAAGAGAATGTCAACCCCGAA-3' and R 5'- AGGAAGGTCCTTAAGAGGAGCAA-3'); *AR* (F 5'-GGTCTTCTTCAAAAGAGCCGCTG-3' and R 5'- TTACGAGCTCCCAGAGTCATCCCT-3'); *PGC1α* (F 5'- CCATACACAACCGCAGTTGC-3' and R 5'- ACCCTTGGGGTCATTTGGTGA-3'); *Igf1* (F 5'- CATGCCCAAGACTCAGAAGTCCC-3' and R 5'-AGGTCTTGTTTCCTGCACTTCCTC-3'); Atrogin-1 (F 5'- GACAAAGGGCAGCTGGATTGG-3' and R 5'- TCAGTGCCCTTCCAGGAGAGA-3'); *Murf-1* (F 5'-TGATTCTCGATGGAAACGCTATGG-3' and R 5'- ATTCGCAGCCTGGAAGATGTC-3'); *Col4a1* (F 5'- AAGGGAGAGCAAGGGGTCAG -3' and R 5'-GTACTCCCGGAAATCCAGGTTCA-3'); *Col4a2* (F 5'- TGGGCCCACAACATCAACGA -3'

and R 5'- AAGGCCAGGAAAACCCCGTA -3'); *Col5a1* (F 5'-CAAGCCAGGTTGGCACTGAG-3' and R 5'- CACCTTTCAAACCGCCACTCC-3'); *Lama5* (F 5'- TTCCCACACTGCTACCCTCTG-3' and R 5'- GTCCCAACCTTGGGTCCTTC-3'); *p16* (F 5'- GCTGCGCTCTGGCTTTCGTGAA -3' and R 5'- TGCCCATCATCATCACCTGGTCCAG -3); *p21* (F 5'- CGGTGTCAGAGTCTAGGGGA -3' and R 5'- AGGATTGGACATGGTGCCTG -3), and *Igfbp5* (F 5'- TACCTGCCCAACTGTGACCG-3' and R 5'-ATCCACGTACTCCATGCCCG-3').

RNA sequencing

RNA was extracted from cultured satellite cells using ISOGEN (Nippon Gene) and RNeasy Mini kit according to the manufacturer's instructions. RNA-Seq libraries were prepared using the TruSeq Stranded mRNA Sample Prep Kit setA (Illumina, San Diego CA) according to the manufacturer's instructions, and were subsequently validated for an average size of approximately 330-340 bp using a 2100 Bioanalyzer and the Agilent DNA1000 kit for the construction of sequencing libraries. Sequence data were mapped on the mouse genome (mm10) using Tophat and analyzed by Cufflinks software (http://cole-trapnell-

112 lab.github.io/cufflinks/). The enrichment of gene ontology was calculated by gene ontology

113 tool Database for Annotation, Visualization, and Integrated Discovery (Huang da et al., 2009a,

114 b).

115

116 **References**

117 Fujita, R., Yoshioka, K., Seko, D., Suematsu, T., Mitsuhashi, S., Senoo, N., Miura, S., Nishino,
118 I., and Ono, Y. (2018). Zmynd17 controls muscle mitochondrial quality and whole-body
119 metabolism. FASEB J *32*, 5012-5025.
120 Huang da, W., Sherman, B.T., and Lempicki, R.A. (2009a). Bioinformatics enrichment tools:
121 paths toward the comprehensive functional analysis of large gene lists. Nucleic acids
122 research *37*, 1-13.
123 Huang da, W., Sherman, B.T., and Lempicki, R.A. (2009b). Systematic and integrative
124 analysis of large gene lists using DAVID bioinformatics resources. Nature protocols *4*, 44-57.
125 Ono, Y., Calhabeu, F., Morgan, J.E., Katagiri, T., Amthor, H., and Zammit, P.S. (2011). BMP
126 signalling permits population expansion by preventing premature myogenic differentiation in
127 muscle satellite cells. Cell death and differentiation *18*, 222-234.
128 Ono, Y., Urata, Y., Goto, S., Nakagawa, S., Humbert, P.O., Li, T.S., and Zammit, P.S. (2015).
129 Muscle stem cell fate is controlled by the cell-polarity protein Scrib. Cell Rep *10*, 1135-1148.
130

131